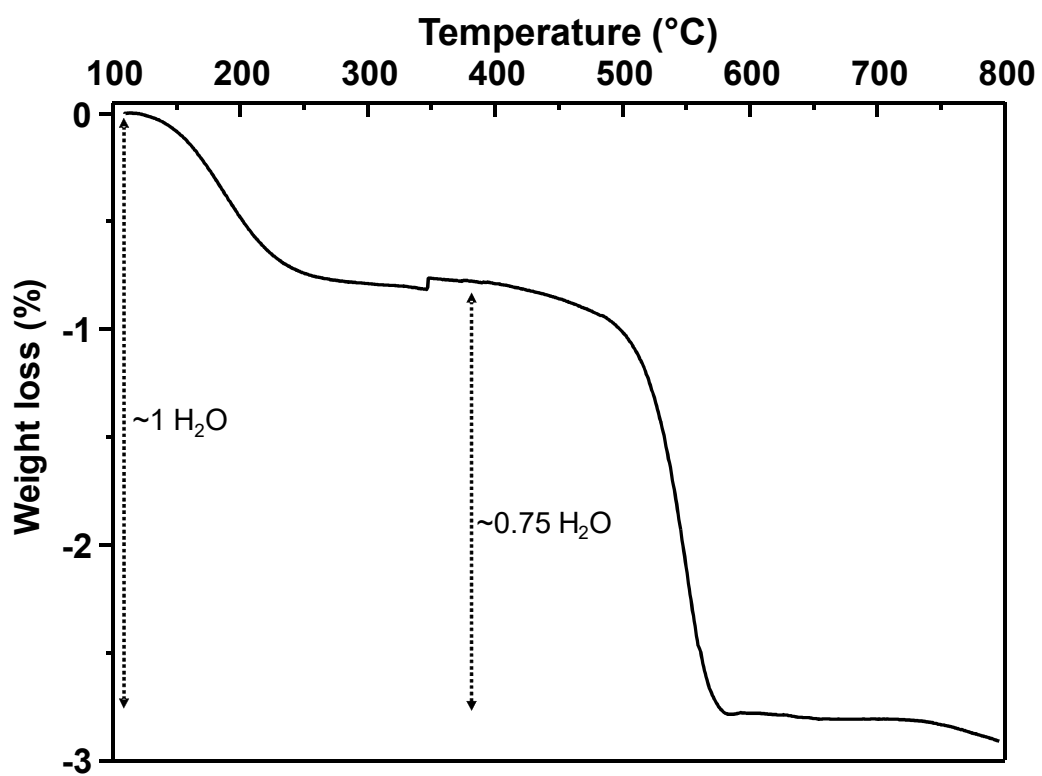
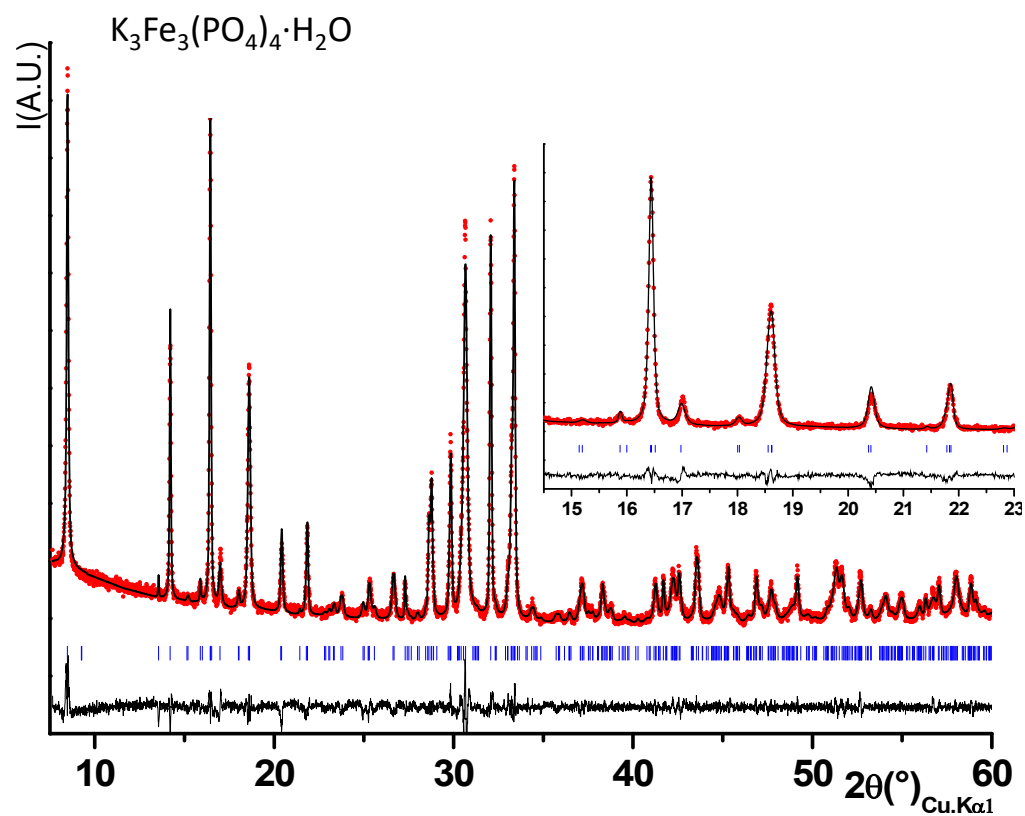


**Figure 1:** X-ray diffraction patterns of  $Na_3Fe_3(PO_4)_4$  and  $K_3Fe_3(PO_4)_4 \cdot H_2O$  after  $Na^+/K^+$  ions exchange in aqueous solution.

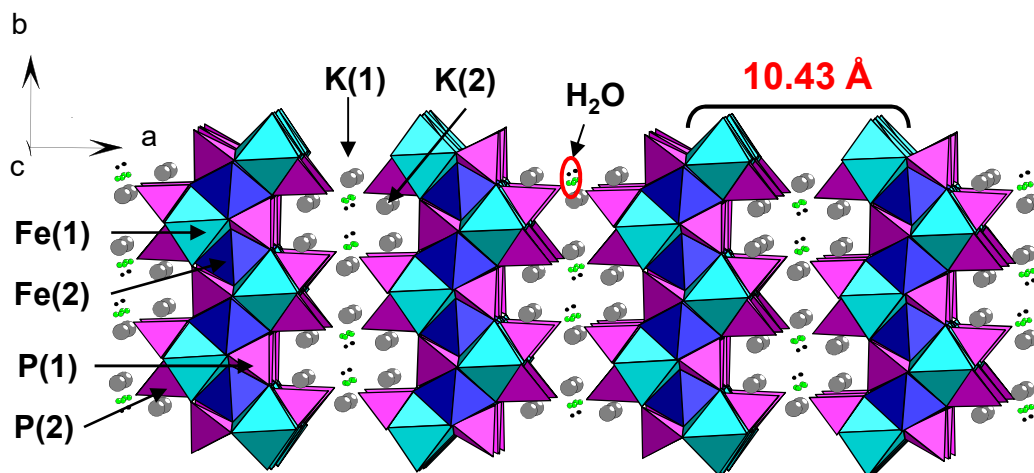


**Figure 2:** Thermogravimetric thermal analysis (TGA) of  $K_3Fe_3(PO_4)_4 \cdot H_2O$  performed under argon flow at  $5^\circ C/min$ .



**Figure 3:** Comparison between the experimental (\*) X-ray diffraction pattern of  $K_3Fe_3(PO_4)_4 \cdot H_2O$  ( $P2/n$ ) and the calculated (-) one using the Le Bail method. The difference plot ( $I_{obs} - I_{calc}$ ) is also given, as well an enlargement of a selected angular range is given to evaluate the quality of the refinement.

a)  $\text{K}_3\text{Fe}_3(\text{PO}_4)_4 \cdot \text{H}_2\text{O}$



b)  $\text{Na}_3\text{Fe}_3(\text{PO}_4)_4$

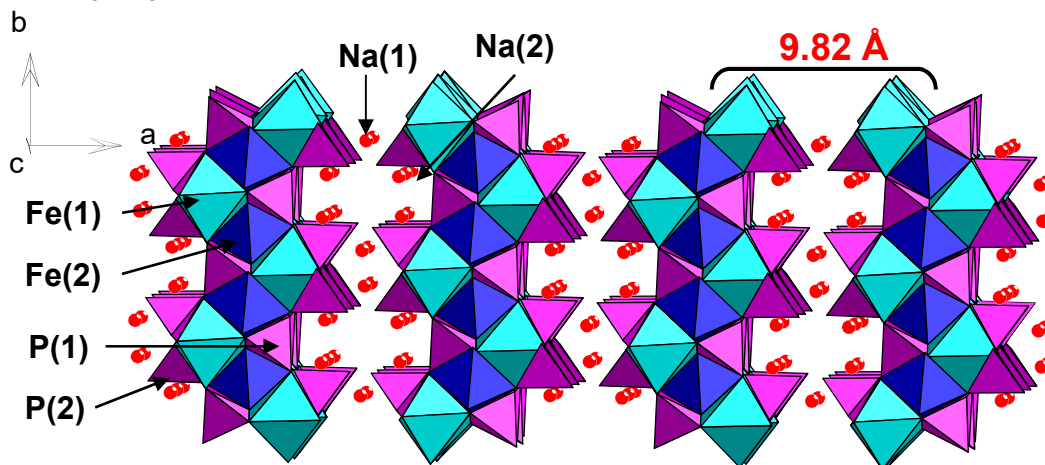


**Figure 4:** Representation of the structures of the  $\text{K}_3\text{Fe}_3(\text{PO}_4)_4 \cdot \text{H}_2\text{O}$  (a) and  $\text{Na}_3\text{Fe}_3(\text{PO}_4)_4$  (b) phases.

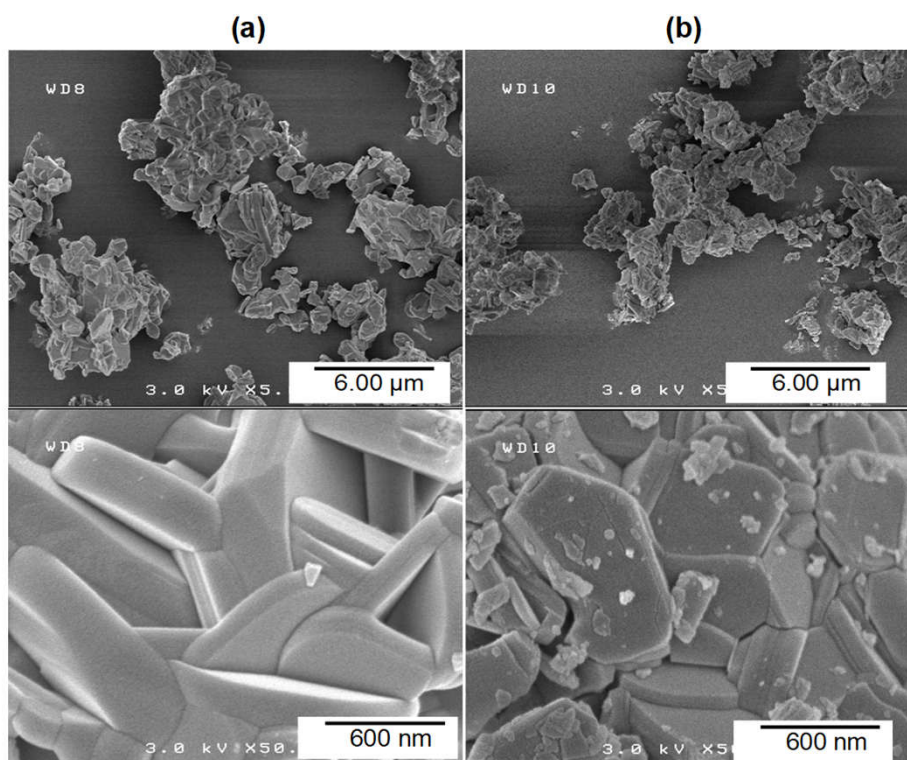


**Figure 5:** SEM micrographs of  $K_3Fe_3(PO_4)_4 \cdot H_2O$  (a) and  $Na_3Fe_3(PO_4)_4$  (b).

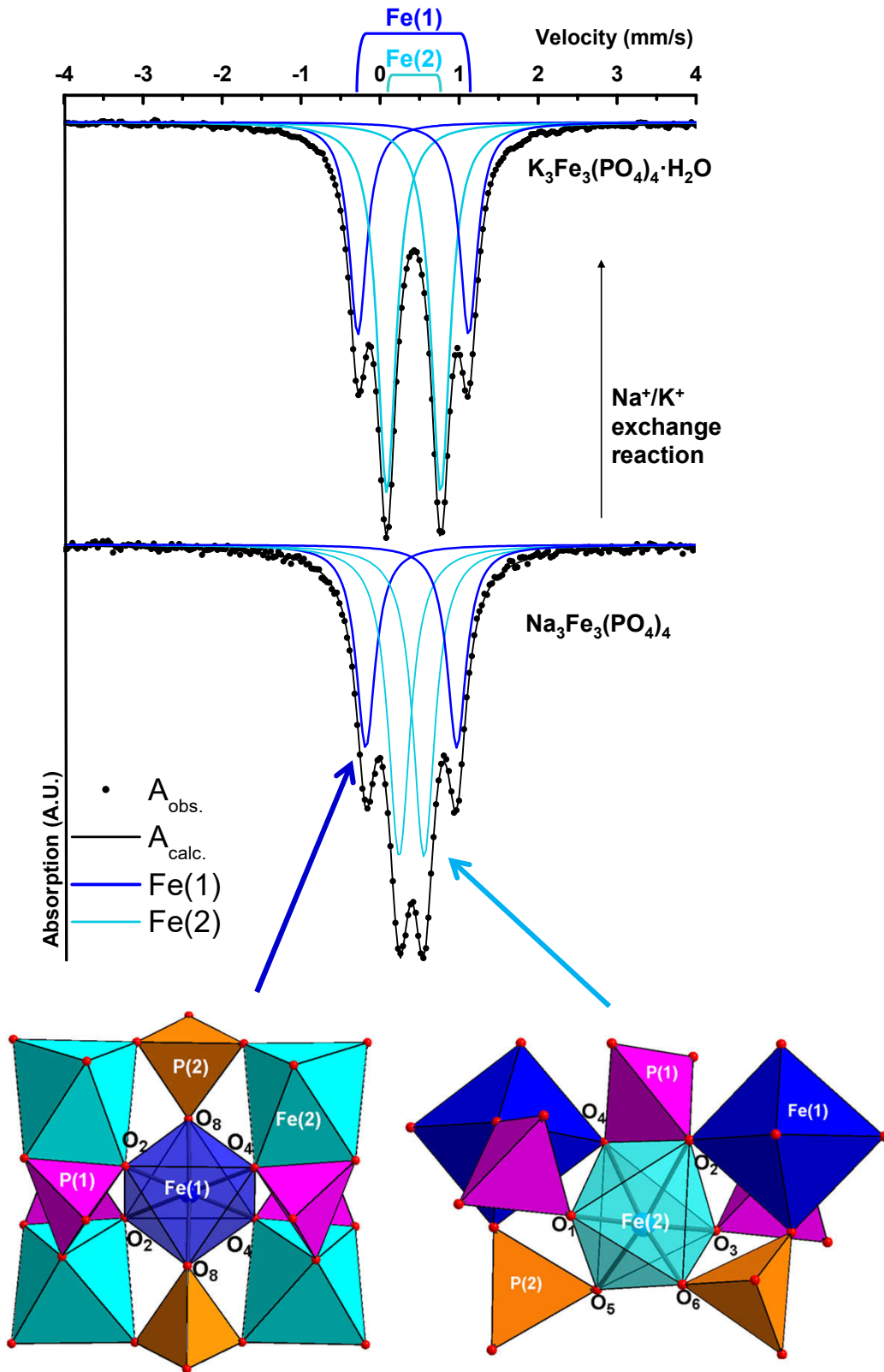


**Figure 6:** Experimental Mössbauer spectra of  $\text{K}_3\text{Fe}_3(\text{PO}_4)_4$  and  $\text{Na}_3\text{Fe}_3(\text{PO}_4)_4$  recorded at room temperature and calculated Lorentzian quadrupole doublets associated to Fe(1) and Fe(2).

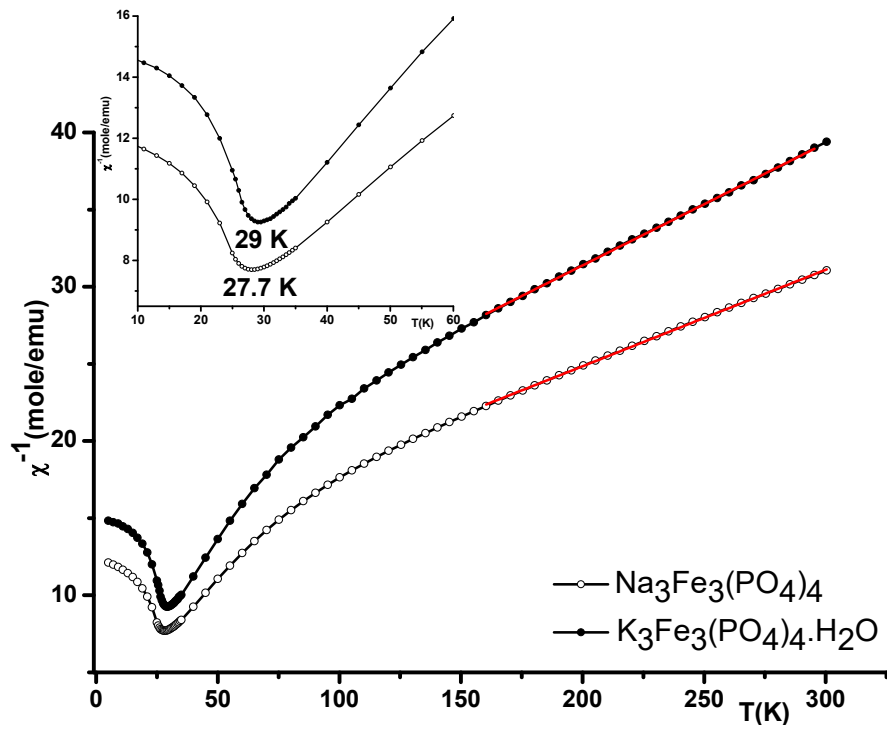


**Figure 7:** A plot of the reciprocal susceptibility versus temperature for  $\text{K}_3\text{Fe}_3(\text{PO}_4)_4 \cdot \text{H}_2\text{O}$  and  $\text{Na}_3\text{Fe}_3(\text{PO}_4)_4$  with an applied field 10 kOe.

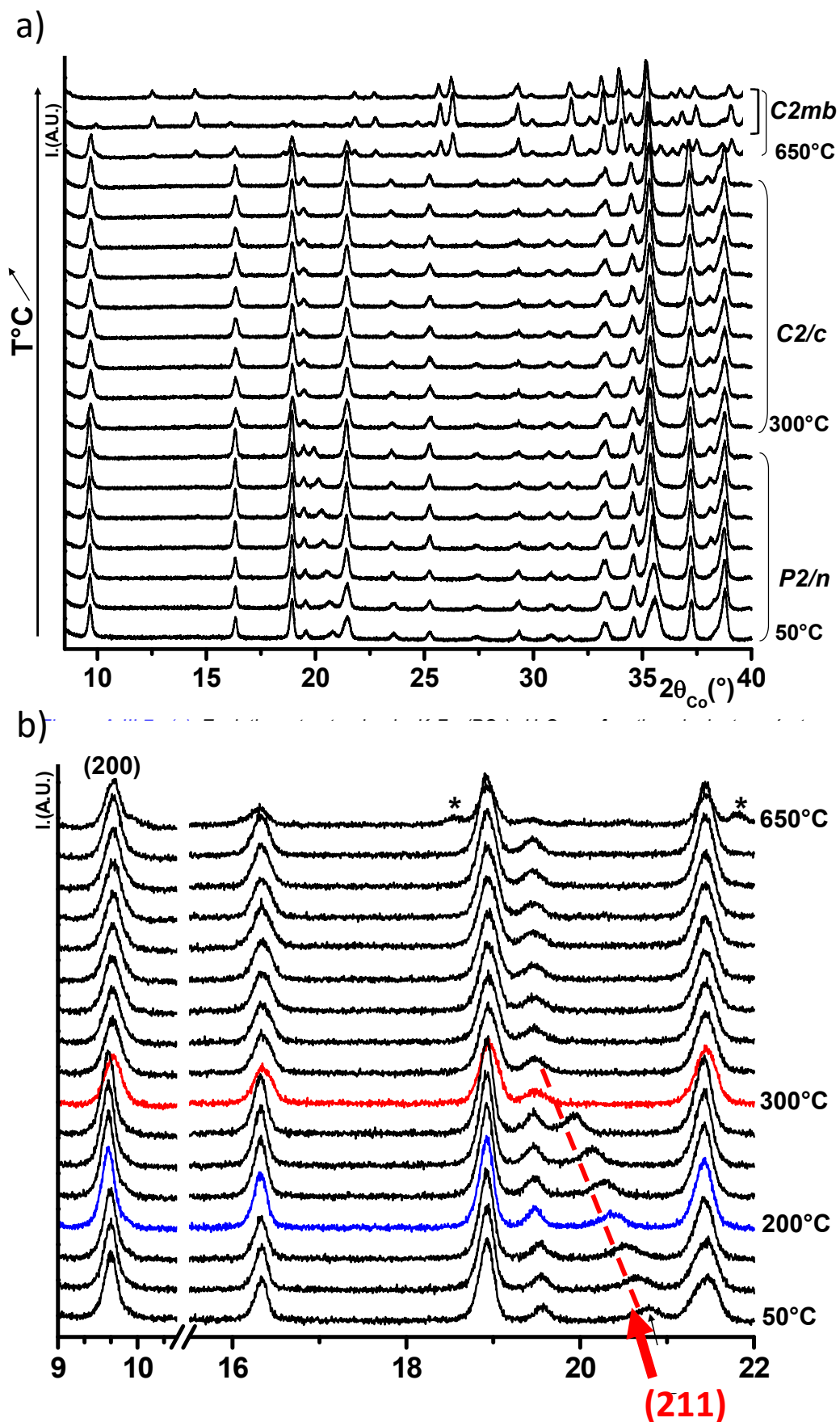


**Figure 8:** *In-situ* XRD patterns recorded while heating  $\text{K}_3\text{Fe}_3(\text{PO}_4)_4 \cdot \text{H}_2\text{O}$  from room temperature to 800°C. a) global view and (b) zoom on specific  $2\theta$  ranges and temperature domain.



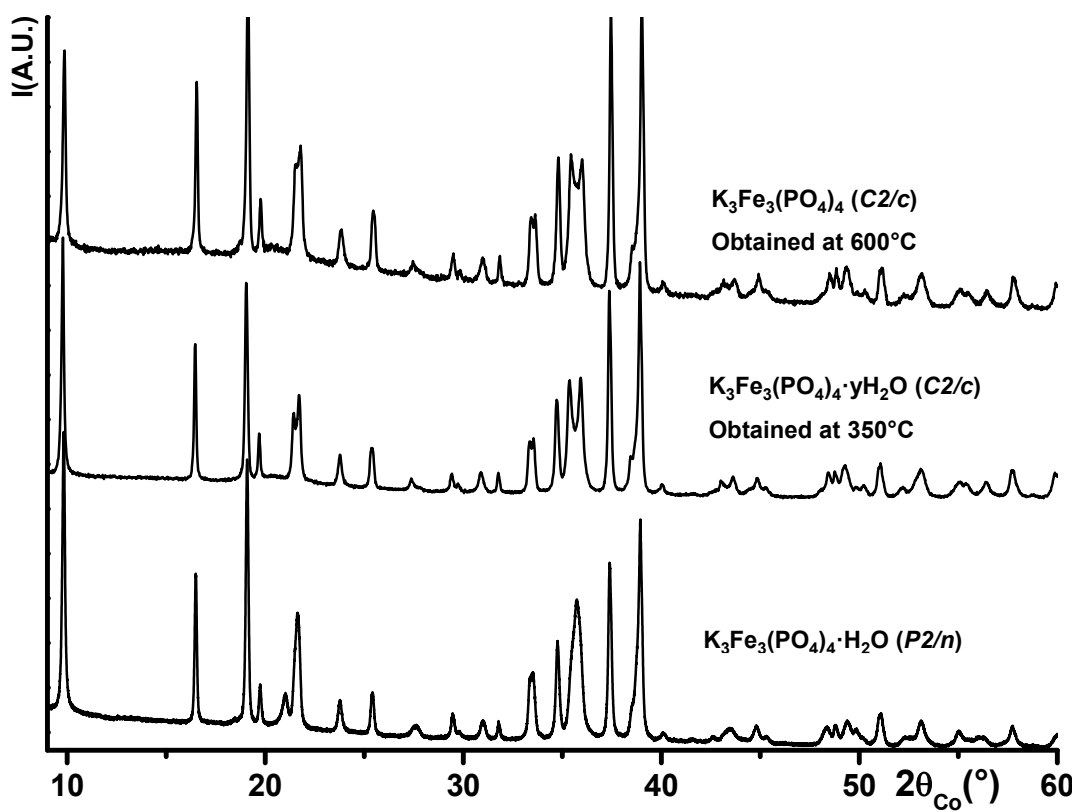


**Figure 9:** *Ex situ* room temperature XRD patterns of the compounds obtained from  $K_3Fe_3(PO_4)_4 \cdot H_2O$  after heat treatment at 350°C and 600°C compared with the one of the parent phase  $K_3Fe_3(PO_4)_4 \cdot H_2O$ .

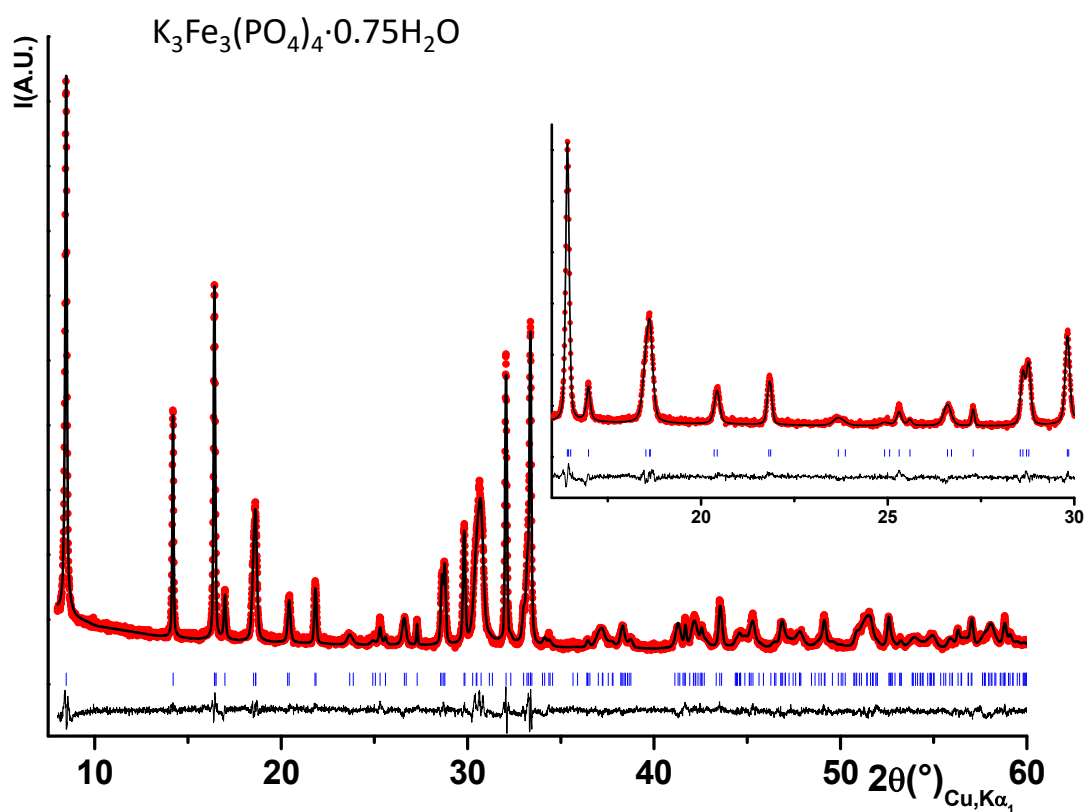


**Figure 10:** Comparison between the experimental (\*) room temperature X-ray diffraction pattern of  $\text{K}_3\text{Fe}_3(\text{PO}_4)_4 \cdot 0.75\text{H}_2\text{O}$  ( $C2/c$ ) obtained at  $350^\circ\text{C}$  and the calculated (-) one using the Rietveld method. The difference plot ( $I_{\text{obs}} - I_{\text{calc}}$ ) is also given, as well An enlargement of a selected angular range is given to evaluate the quality of the refinement.

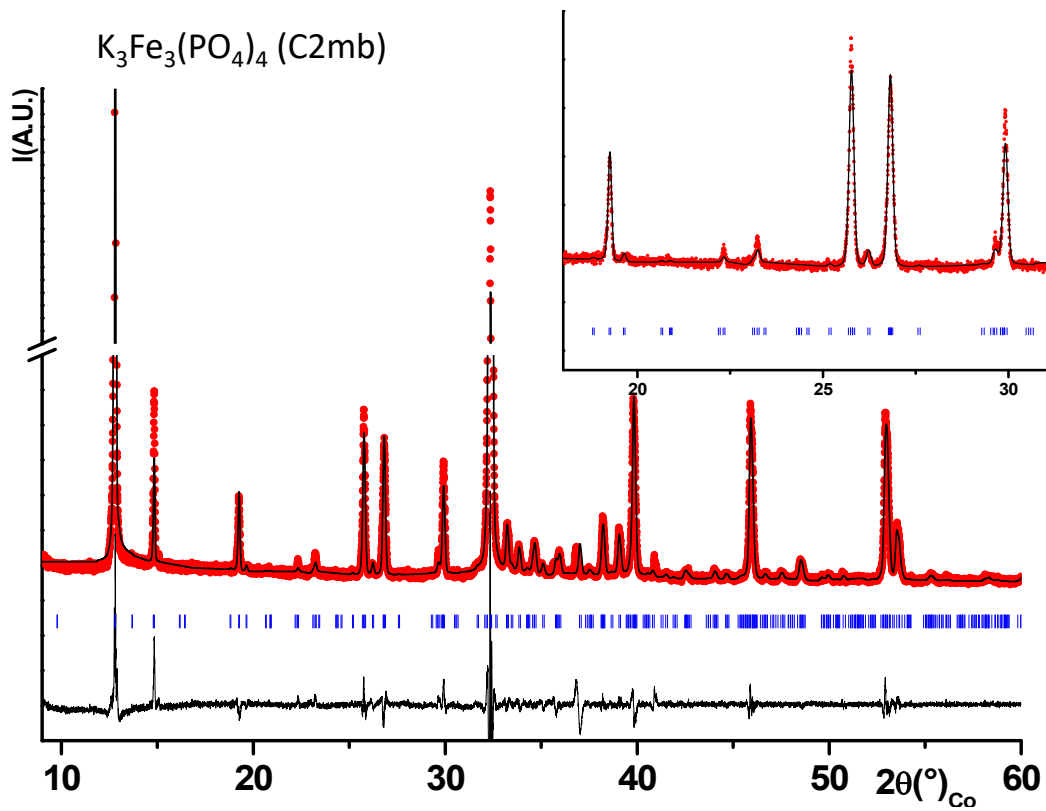


**Figure 11:** Comparison between the experimental (\*) X-ray diffraction pattern of  $K_3Fe_3(PO_4)_4$  (C2mb) obtained at  $750^{\circ}C$  and the calculated (-) one using the Rietveld method. The difference plot (Iobs. – Icalc.) is also given, as well An enlargement of a selected angular range is given to evaluate the quality of the refinement.